Appl. Phys. B 55, 250–257 (1992)

Applied Physics B Photophysics and Laser Chemistry

Quantum Correlated Twin Beams

J. G. Rarity[1], P. R. Tapster[1], J. A. Levenson[2], J. C. Garreau[2], I. Abram[2], J. Mertz[3], T. Debuisschert[3], A. Heidmann[3], C. Fabre[3], and E. Giacobino[3]

[1] Defence Research Agency, Royal Signal and Radar Establishment, St. Andrews Road, Malvern, Worcestershire, WR14 3PS, UK
[2] Centre National d'Etudes des Télécommunications, 196 Avenue Henri Ravéra, F-92220 Bagneux, France
[3] Laboratoire de Spectroscopie Hertzienne, Université P.M. Curié, B.P. 74, F-75252 Paris 05, France
(Fax: +33-1/4427-3845)

Received 23 March 1992/Accepted 2 June 1992

Abstract. We discuss recent progress in the study of the non-classical properties of light beams generated by non-degenerate parametric splitting in $\chi^{(2)}$ nonlinear birefringent crystals, with special emphasis on their quantum correlation ("twin beams"). We describe experimental results using successively pure parametric fluorescence, parametric amplification of a weak signal beam pumped by a pulsed laser, and parametric oscillation in a cavity pumped by a cw laser. In this review, we compare the respective advantages and drawbacks of the different approaches.

PACS: 42.50.Dv, 42.65.Ky

Sensitivity in optical measurement was, until recently, considered to be ultimately limited by the shot noise limit (SNL) obtained using classical coherent states. The production of non-classical light, in which the fluctuations of photon number or the amplitude of one quadrature component, is reduced below that for a classical coherent state has changed that view. The antibunched nature of single atom fluorescence was demonstrated in the first nonclassical light experiments [1] and later shown to be weakly sub-Poissonian [2]. Four-wave mixing near resonance in sodium vapour provided the first demonstration of phase squeezing [3]. Noise reduction of a few percent below the classical limit was demonstrated in one field quadrature but absorbtion in the wings of the atomic resonance prevented large noise reduction. The limitations of these atomic sources led to study of experiments based on $\chi^{(2)}$ non-linearities in a variety of birefringent crystals. Such crystals can be highly transparent in the near infrared and their development has, in the past, been driven by potential frequency doubling applications. However, when pumped by short wavelength lasers, output light at (or around) the half-wavelength is generated. This parametric downconversion can be thought of simply as a source emitting photons in pairs satisfying energy conservation and phase matching conditions in the crystal. In the degenerate mode pairs cannot be separated and the process is more easily thought of in terms of parametric amplification with one phase quadrature amplified at the expense of the other. Used as degenerate parametric amplifiers such crystals have been shown to be near ideal sources of quadrature squeezed light [4, 5].

In non-degenerate parametric downconversion the pairs can be separated leading to two beams with identical photon statistics. Twin beams of this type were first identified some twenty years ago by photon counting coincidence measurements [6]. However, it was not until the early eighties that it was realised that the detection of photons in one beam could be used to modify the statistics of the other. This led to the demonstration of one photon (Fock) states [7], antibunching [8] and sub-Poissonian light [9]. Due to the limited efficiencies and maximum count-rate of single photon counting detectors, such sources are only slightly sub-Poissonian, providing a flux of some tens of photons per second. Although not useful for practical noise reduction, these single photon counting experiments have led on to the study of various novel quantum interference effects which may have applications in low light level and secure communications [10–12]. The high efficiency of silicon and InGaAs PIN photodiodes in the near infrared has been exploited in recent experiments to show strong noise correlations between the intensities of the signal and idler modes emitted by parametric fluorescence. Higher output powers for the signal and idler beams are achieved when pulsed laser sources are used for cavity free parametric generation. The high instantaneous power levels can lead to large parametric gain allowing pulsed twin beams to be generated from a low power seed beam [13]. Another successful technique consists in using a resonant cavity to recirculate the different interacting fields and generate strongly correlated twin beams at milliwatt power levels [14, 15]. In all the previously mentioned experiments, it is possible to use the fluctuations measured on one beam to correct the fluctuations on the other leading to sub-Poissonian or sub-shot-noise light sources [16, 17].

In this review we present current experimental progress in each of these routes to the generation of correlated twin beams, performed in the three European laboratories (RSRE, ENS, CNET) which are linked by the European ESPRIT basic research action joint project on quantum noise reduction

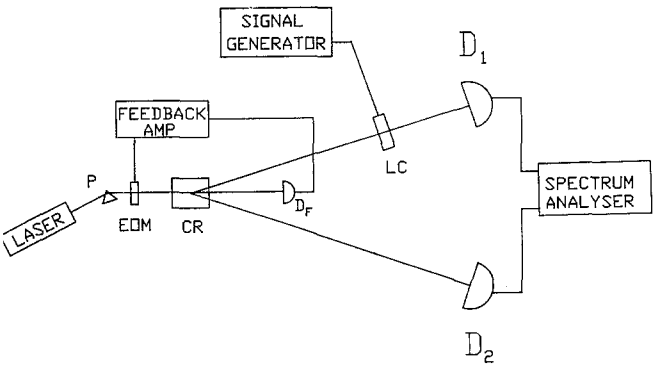

Fig. 1. Schematic diagram of the parametric fluorescence twin beam source. The laser illuminates a lithium iodate crystal (CR) producing twin correlated beams. A liquid crystal cell LC is placed in one of the beams and its transmission modulated using a signal generator. Detectors D_1 and D_2 view the twin beams and their outputs are analysed in a Fourier transform spectrum analyser. The 413.4 nm laser line is selected by a prism (P). Laser noise is reduced by a feedback loop involving detector D_F a feedback amplifier and an electro-optic modulator (EOM)

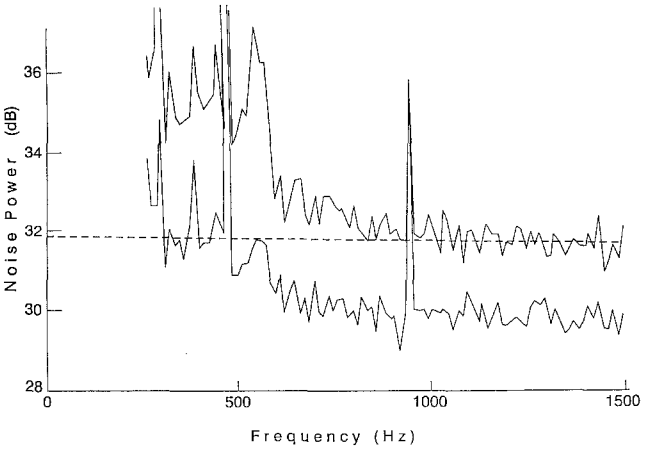

Fig. 2. Measured noise spectra. Upper solid line: Voltage noise (referred to 1 $(\mu V)^2$/Hz and amplifier gain 1.13 GΩ) measured in channel 1 as a function of frequency. Lower solid line: Voltage noise in the difference voltage $\Delta V_1 - k\Delta V_2$ with $k = 0.66$. Dashed line: shot noise level for channel 1

in optical systems. Our main aim is to allow for a precise comparison of the advantages and drawbacks of these different experimental techniques.

1 Twin Beams from Parametric Fluorescence

At the Royal Signal and Radar Establishment, it has been experimentally shown that twin beams generated by parametric fluorescence and selected by phase matching angles were correlated to within 0.7 of the ideal level, the measured photocurrents being on the order of 4 nA. We describe in this section a simple demonstration experiment using such twin beams where the signal to noise ratio in a measurement of turbidity in a weakly scattering sample has been improved by 2 dB on the single beam shot-noise limit (with up to 4 dB possible in situations where classical technical noise is present).

One projected use for twin beam light is in improving the accuracy of transmission measurements (in absorption spectroscopy for example [18, 19]). In certain biological or light sensitive samples a maximum absorbed dose limit will exist, limiting the accuracy with which a measurement of the absorption can be performed. Phase (quadrature) squeezed light can be used to reduce the noise to below the shot-noise limit in such measurements [20] but it is easier in this purpose to exploit the amplitude correlation of twin beams obtained from the non-degenerate parametric downconversion process [19, 21].

A schematic of the apparatus is shown in Fig. 1. An amplitude stabilised krypton-ion laser producing 400 mW of 413.4 nm wavelength light is weakly focussed into a lithium iodate nonlinear crystal. The crystal axis is tilted so that phase matched 826.8 nm light is emitted in a cone of half angle 10°. Correlated beams are selected by placing 2 cm diameter t apertures centred on the 826.8 nm emission at opposite ends of a cone base diameter 1.5 m from the crystal. The resulting beams were broad band (approximately 60 nm bandwidth). Both beams are focussed using anti-reflection (AR) coated lenses through AR coated colour glass filters (cut-on > 750 nm) onto PIN photodiodes D_1 and D_2. These are connected to low noise transimpedance amplifiers with gains of $R_1 = 1.13\,\mathrm{G\Omega}$ and $R_2 = 1.01\,\mathrm{G\Omega}$, respectively. The current noise of the amplifiers and detectors was small compared with the typical shot-noise levels measured. The outputs of the two detector amplifiers were connected via low pass filters (2.5 kHz corner frequency) to an analogue to digital converter and an HP 300 series computer operating as a spectrum analyser.

This apparatus was used to demonstrate the potential signal to noise gains in simple transmission measurements. A sample consisting of a liquid crystal cell with mean transmission coefficient $\alpha = 0.85$ was placed in front of detector D_1 (see Fig. 1) and its transmission was weakly modulated at 480 Hz and 960 Hz by applying a low voltage sine wave across the cell.

The computer calculated noise voltage spectra $\langle \Delta V_i^2 \rangle$ $(i = 1, 2)$ and the voltage difference spectra $\langle (\Delta V_1 - k\Delta V_2)^2 \rangle$ of the detector amplifier outputs with feedback parameter k set either for optimum quantum noise reduction or for maximum classical noise rejection. For optimum quantum noise reduction [18]

$$k = \alpha\eta_1 R_1 / R_2 \tag{1}$$

(η_1 and η_2 are the effective efficiencies, including optical losses, of channels 1 and 2). In this case the voltage noise referenced to the single beam shot-noise limit is given by

$$\frac{\langle (\Delta V_1 - k\Delta V_2)^2 \rangle}{2e^2 r \Delta f \alpha \eta_1 R_1^2} = (1 - \alpha\eta_1\eta_2)\,, \tag{2}$$

where e is the electron charge, r is the pair photon rate at the crystal, and Δf is the resolution of the spectrum analyser. The result of a measurement with detected photocurrents of 3.4 nA and using $k = 0.66$ is shown in Fig. 2 along with the uncorrected voltage noise spectrum which reaches the shot-noise limit above 800 Hz. Clearly, the background noise level of the difference spectrum drops some 2 dB below the

shot-noise limit for measurements at 960 Hz. Around the 480 Hz fundamental, the classically correlated noise is not fully removed. This noise is minimised by choosing

$$k = R_1 \alpha \eta_1 / R_2 \eta_2 \,. \tag{3}$$

For our situation $\alpha\eta_1/\eta_2 \approx 1$ and $k = 1.12$ was used to produce the noise spectrum shown in Fig. 3. Suppression of classical noise is now seen around the 480 Hz fundamental signal (shown by the total disappearance of the 500 Hz noise peak seen in both traces of Fig. 2). The shot-noise level that would be obtained using classical balanced subtraction is shown. For this case the theory predicts a noise referenced to the two beam shot-noise limit

$$\frac{\langle (\Delta V_1 - k\Delta V_2)^2 \rangle}{3e^2 r \Delta f \alpha \eta_1 R_1^2} = (1 - \alpha\eta_1) \tag{4}$$

when $\alpha\eta_1/\eta_2 \approx 1$ and $k = R_1/R_2$. Figure 3 clearly shows some 4 dB of noise reduction below this theoretical shot-noise limit (verified in a separate experiment where the crystal was replaced by a tungsten bulb of equal intensity). It must be emphasised that 4 dB is only gained when the single beam measurement is not shot-noise limited.

The limitations to the measured noise reductions are detector efficiencies ($\eta \approx 0.85$), optical losses in each channel (transmission efficiency ≈ 0.95) and background amplifier noise ($\approx 10\%$ of measured noise). These known losses lead to an effective detector efficiency of ≈ 0.73 which coupled with the sample transmission of $\alpha = 0.85$ leads to a noise reduction to 0.4 of the shot-noise level or a noise reduction of 4 dB as measured. Improved detectors (to 95% efficiency), a higher sample transmission and lower noise amplifiers could improve the measurement to give near 10 dB noise reduction. It must be noted that the maximum noise reduction even with ideal detection will be ultimately limited to $1 - \alpha$, which is the fraction of light lost in the sample.

2 Pulsed Parametric Light

The high intensities provided by mode-locked and/or Q-switched lasers permit the implementation of efficient travelling-wave parametric amplifiers, without the need to build a resonant optical cavity around the nonlinear medium to achieve high parametric gains. Parametric gains of the order of 100 dB can be attained [22] so that the spontaneously generated parametric photons at the entrance of the nonlinear crystal can be amplified in the course of their propagation through the crystal, to produce pulses of megawatt peak power. At such high gains, however, the quantum noise of the parametic pulses is masked by the classical intensity and phase fluctuations that are produced by the gain instabilities due to the variations of the pump pulse. In particular, the small variations of the pump phase prevent, generally, the observation of the de-amplified quadrature in the parametric signal. Nevertheless, even the classical noise of megawatt parametric pulses displays correlations that attest to the twin-photon quantum origin of the parametric emission process [23]. At lower gains, of the order of 10–20 dB, the classical fluctuations of the parametric amplifier should be better controlled, and quantum noise effects, such as squeezing or twin photons should be directly accessible.

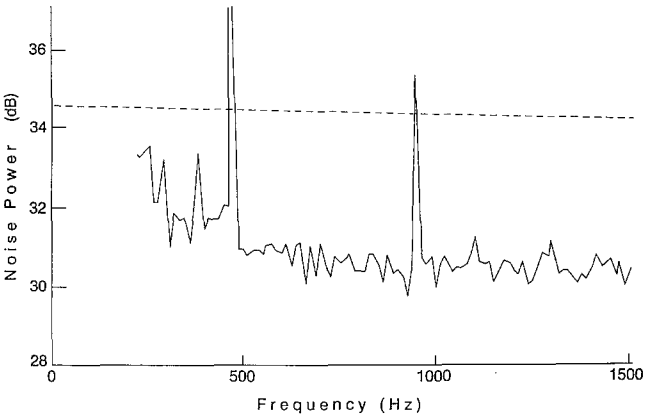

Fig. 3. Measured noise spectra; Solid line: Voltage noise in the difference voltage $\Delta V_1 - k\Delta V_2$ with $k = 1.12$. Dashed line: shot-noise level for channel 1 plus channel 2

The gain and noise characteristics of a travelling-wave parametric amplifier are quite different from a parametric amplifier using an optical cavity. In particular, since there is no cavity to filter the field fluctuations, the squeezed light and the twin photons produced in a travelling-wave configuration are broad-band and their spectrum extends, in principle, to the THz region. On the other hand, in the absence of the spatial filtering effect introduced by the cavity, the Gaussian spatial profile of the pump produces a strong spatial variation of the parametric gain in the transverse direction. This introduces a coupling in the signal between its fundamental (Gaussian) mode and its higher-order transverse modes. At the same time, the short-pulse nature of the pumping process implies that the gain of the parametric amplifier varies in the course of time in a way that follows the temporal profile of the pump pulse. This also introduces a distortion of the temporal profile of the amplified and de-amplified quadratures of the signal, analogous to that of the spatial mode mixing. The measurement of squeezing in such a case requires the use of an appropriately matched local oscillator, so as to compensate the mode distortions [24].

At low peak gains, of the order of a few dB, travelling-wave parametric amplification and de-amplification may be considered to be uniform, and under such conditions squeezing has been observed [5, 23, 25]. At higher gains, however, the signal mode is strongly distorted and its amplified and de-amplified quadratures assume non-Gaussian (and different) profiles [26]. The reduction of quantum noise in the squeezed quadrature quickly saturates as anti-squeezed components from higher-order modes start coming in. Twin photons, on the other hand, have been observed with parametric gains of up to 10 dB [13]. The reason that twin photons are less sensitive to the gain distortions is that their observation usually involves operation of the parametric amplifier in a phase-insensitive configuration. Thus, the de-amplified quadrature, which suffers most of the distortion, is not probed in twin photon experiments. In preparing for the measurement of quantum noise correlations in high-gain parametric amplification, we carried out preliminary experiments to determine the techniques that are best suited for the observation of twin photons and squeezing in pulsed parametric light. In these experiments we examined the amplification and de-

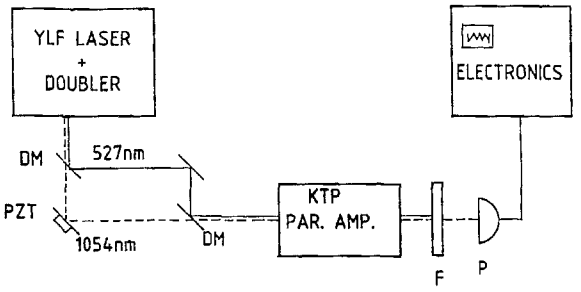

Fig. 4. Experimental setup for high-gain pulsed parametric light. DM = Dichroic mirror; F = Infrared filter; P = Photodiode; PZT = Piezo-electric translator

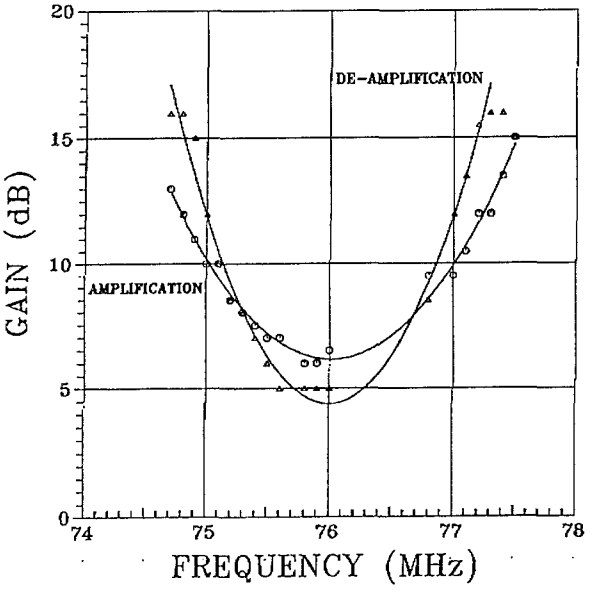

Fig. 5. Absolute values of the gain in the spectral components of the amplified and de-amplified quadratures of the probe train envelope. Parabolae are drawn as a guide to the eye. Gain imbalance between the two quadratures is due to the high-gain distortion of the envelope

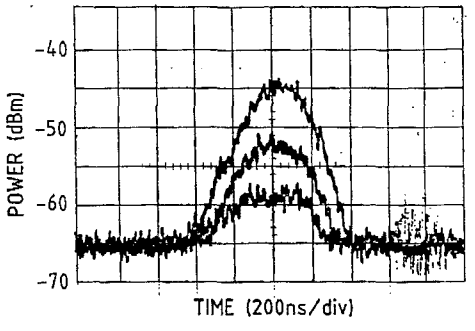

Fig. 6. Temporal profile of the intensity of the probe train envelope (central trace), of its amplified quadrature (upper trace) and of its de-amplified quadrature (lower trace). Note amplification and de-amplification gains are balanced throughout the envelope profile

amplification of a classical signal traversing a pulsed parametric amplifier. Spatial filtering techniques were used to reduce the effects of spatial distortion, and thus examine only the distortion of the temporal profile.

The travelling-wave parametric amplifier consists of a nonlinear KTP crystal pumped by an intense beam at 527 nm, which is obtained by frequency doubling the output of a mode-locked and Q-switched Nd:YLF laser. A block diagram of the experimental setup is given in Fig. 4. The pump beam consists of 440 ns-long (FWHM) trains of 35 ps-long pulses, with a Gaussian train envelope, produced at a repetition rate of 1 kHz. In each train, the pulses are separated from each other by 13.2 ns. In the KTP crystal, the central pulses in the train have a peak intensity of the order of 100 MW/cm^2, producing a parametric gain of up to 15 dB. A small portion of the infrared light (at 1054 nm) emerging from the laser is also injected in the KTP crystal co-linearly with the pump beam and serves as a probe for the amplification process. The probe beam consists of 630 ns-long trains of pulses, synchronized with the pulses of the pump beam. The optical phase between the pump and the probe is scanned by means of a piezoelectric translator (PZT).

One of the limitations of conventional frequency-domain measurements, such as those described in Sect. 3, when applied to short pulse trains, lies in the fact that spectral analysis essentially averages over parts of the train envelope that have widely different gain and noise characteristics. The envelope distortions are translated into spectral changes that do not reflect in a direct way the parametric gain. This is illustrated in Fig. 5 which represents the gain measured in the spectral profiles of the amplified and de-amplified quadratures of the probe. The spectra are centered at 76 MHz, the repetition frequency of the mode-locked pulses, and are taken with a resolution bandwidth of 300 kHz. The nominal gain for amplification and de-amplification is 7 dB. At the central frequency the measured gain is near the nominal value, but there is a slight gain imbalance between the two quadratures (7 dB vs −5 dB). On the spectral wings, on the other hand, the apparent gain is higher and displays a stronger imbalance between the two quadratures (11 dB vs −15 dB). These features, however, correspond essentially to the high-frequency distortion of the time-profile of the envelope.

Figure 6, on the other hand, is the superposition of three *temporally-resolved* intensity profiles of the probe train envelope at the exit of the parametric amplifier. The central trace corresponds to the absence of amplification (gain = 0 dB), while the upper and lower traces represent, respectively, the amplified and de-amplified quadratures of the probe. The gain at the peak of the envelope is 7 dB and follows essentially a parabolic temporal profile that reflects the Gaussian pump envelope. Note that the amplified and de-amplified quadratures are not Gaussian, but are strongly distorted, with the de-amplified envelope exhibiting a "hole" in the center due to the strong local de-amplification, as discussed also by LaPorta and Slusher [26]. Nevertheless, as can be seen in this figure, at all points in time the amplification and de-amplification gains are equal. Since the de-amplified quadrature is also the one that exhibits squeezing, the observation of balanced gains throughout the envelope profile implies that time-resolved measurements of quantum noise will not be affected by the high-gain distortions of the probe. However, if the temporal resolution of the apparatus is insufficient it will average regions with widely different gains and produce an apparent saturation of de-amplification and of squeezing.

These experiments on the classical gain of the parametric amplifier demonstrate that time-resolved measurements, rather than spectral analysis, are a more appropriate technique for pulsed work, underscoring the fact that the parametric gain depends on the instantaneous intensity of the pump and is not local in frequency-space. Similar considerations apply also to the quantum noise characteristics of pulsed parametric light. Time-resolved experiments on the quantum noise correlations (twin photons and squeezing) of pulsed parametric light are presently under way.

3 Twin Beams from Optical Parametric Oscillators

To enhance nonlinear effects in the $\chi^{(2)}$ in the cw regime, it is possible to insert it in an optical cavity. One then obtains an optical parametric oscillator (OPO), which can be either doubly resonant (DROPO) when the cavity finesse is high only for the signal and idler modes, or triply resonant (TROPO), when the cavity build-up is important for the signal, idler and pump modes at the same time. The twin character of the signal and idler photons emitted in the parametric crystal still remains in the output fields, but the presence of the cavity introduces significant differences as compared to the previously described situation of parametric fluorescence.

(1) Because of the feedback effect induced by the cavity, the dynamical behaviour of the system is changed, and becomes in a way similar to the one of a laser. Below a pump threshold intensity I_t, there is no mean output field generated in the signal and idler modes by the OPO, whereas above this value, non-zero mean fields are produced at the signal and idler frequencies. This threshold I_t is given by:

$$I_t = \frac{(1-r_0)(1-r_1)(1-r_2)}{\chi^2(1++r_0)r_1r_2}, \tag{5}$$

where r_0, r_1, and r_2 are the amplitude reflection coefficients, respectively, for the pump, signal and idler modes. χ is a coefficient characterizing the three-wave mixing in the crystal, and depending on the crystal nonlinear coefficient, the overlap between the three coupled modes, and phase matching conditions. Let us mention that one can also encounter situations where the system becomes bistable or unstable [27].

(2) The cavity acts as a filter for both longitudinal and transverse properties of the emitted fields, playing in this respect the role of the filters and apertures used in the experiments described in the previous part. Above threshold, the OPO generates output beams in modes which are combinations of the transverse eigenmodes of the optical cavity, depending on the different resonance conditions for the different transverse modes. Using a suitably focussed pump beam, it is possible to operate an OPO in the TEM_{00} mode for the signal and idler fields.

As far as the longitudinal properties are concerned, and in the case of DROPO, two resonance conditions must be fulfilled at the same time:

$$\omega_1 L_1/c = 2\pi p_1, \qquad \omega_2 L_2/c = 2\pi p_2, \tag{6}$$

where ω_1, ω_2 are the frequencies and L_1, L_2 the optical lengths for the signal and idler modes. L_1 and L_2 can be different because of dispersion or, in a type-II crystal, because of birefringence. p_1 and p_2 are integer numbers. As a result, only a discrete series of values for the geometrical length L of the optical cavity is suitable for OPO operation. Actually, resonance conditions (6) are not absolute, because the OPO can oscillate with frequencies slightly detuned from the perfect resonance conditions (but the detunings for the signal and idler modes have to be identical [27]). The values of L for which the oscillation takes place form finite intervals around the values obtained from (6), the spacing between the intervals being proportional to the difference between the indices of refraction for the signal and idler modes, $n_1 - n_2$ [28, 29].

In the case of TROPO, an additional resonance condition must also be satisfied:

$$\omega_0 L_0/c = 2\pi p_0, \tag{7}$$

with notations similar as in (6), but for the pump mode. Therefore, to obtain simultaneous triple resonance, one needs an extra control parameter to be scanned, which can be either the pump frequency ω_0, or some variable acting on the three indices of refraction and therefore on the three optical paths L_i (angle, temperature, electrostatic field applied on the crystal). Taking into account the possibility of detunings, one finds that in the TROPO case, the threshold for OPO oscillation is modulated by the Airy function describing the intracavity pump build-up. The different finesses can then be chosen in such a way that there is at least one peak of the series fulfilling (6) within a pump resonance peak. In such a situation scanning the length is sufficient to get the TROPO operation. The tuning of another control parameter is nevertheless useful in order to get the maximum output power from the device.

(3) The last effect of the cavity is to filter the fluctuations of the various fields. In consequence, the range of noise frequencies in which the outgoing fields have quantum fluctuations departing from the shot-noise level is limited to the cavity bandwidth (and similar noise intervals around multiples of the cavity free spectral range [30, 31]), whereas it was only limited by less stringent phase matching considerations in the case of parametric fluorescence described in Sects. 1 and 2. The twin character of the signal and idler beams appears in the noise reduction existing in the difference $I = I_1 - I_2$ between the intensities of the signal and idler beams. The noise spectrum $S_I(\Omega)$ of this quantity, normalized to shot-noise, is given, in the balanced case (same transmission and losses for the signal and idler modes) by the expression [32]:

$$S_I(\Omega) = 1 - \frac{\xi\eta}{1+\Omega^2/\Delta^2}, \tag{8}$$

where Δ is the cavity bandwith, η is the detection quantum efficiency, and ξ is the OPO coupling efficiency, given by:

$$\xi = \frac{T}{T+L}. \tag{9}$$

$T = 1 - r_1^2 = 1 - r_2^2$ is the coupling mirror transmission coefficient for the signal and idler modes, and L the extraneous cavity loss coefficient for the signal and idler modes. One will find in [33–36] a detailed analysis of all the fluctuation spectra for the signal, idler, and reflected pump fields.

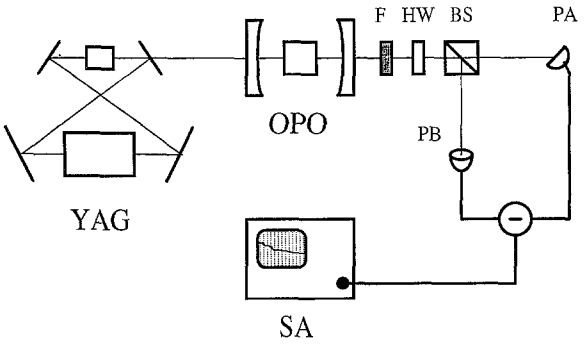

Fig. 7. Experimental setup for twin beam generation using intracavity parametric interaction. The optical parametric oscillator is pumped by an intracavity doubled ring YAG laser. The transmitted pump beam is blocked by filter F. The signal and idler beams are separated by a polarizing beamsplitter BS and measured by high efficiency photodiodes PA and PB (HW: half-wave plate; SA: spectrum analyser)

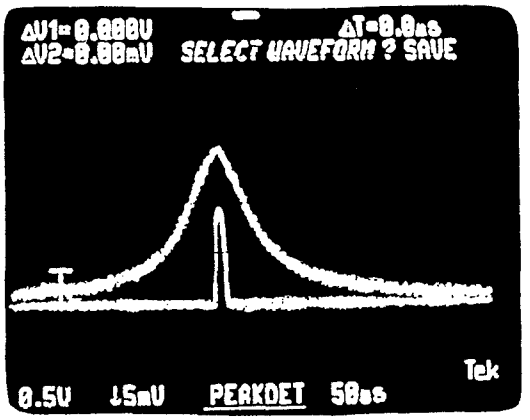

Fig. 8. Intracavity pump mean intensity (top curve) and signal output power (bottom curve) as a function of swept cavity length. The triple resonance condition is fulfilled in a small length interval (about 3 nm) lying in an Airy resonance peak for the pump field in the OPO cavity

Let us now describe the experiment performed at the Laboratoire de Spectroscopie Hertzienne. We will give here a complete description of the experimental setup, already outlined in [32]. It is sketched in Fig. 7. A single mode, cw, intracavity doubled, ring Nd:YAG laser, of typical power 400 mW at 532 nm, is used as a pump. It is focussed into the OPO cavity, which has a length of 35 mm and is limited by mirrors of radii of curvature 20 mm. The parametric medium is a 10 mm long KTP crystal, AR coated for 1064 and 532 nm, and cut to obtain optimum type II phase matching conditions for the frequency doubling of 1064 nm light. Its temperature is stabilized to 26.6° C. The beam waist in the crystal is approximately equal to 50 μm. The signal and idler waves, almost degenerate in frequency, are cross polarized, with different indices of refraction ($n_e = 1.746$, $n_o = 1.833$) and a walk-off inside the crystal of 1.3 mrad. As a result, the signal and idler output beams have a small angular divergence of 3 mrad. The relative difference between the two beam mean intensities is less than 2%. The sum of the signal and idler beam intensities is stabilized in the mW range by adjusting the OPO cavity detuning through piezoelectric control of the cavity length (bandwidth of control: 1 kHz). It was found experimentally that the OPO intensity servo-control was sufficient for stable OPO operation, without resorting to any stabilization of the pump laser frequency.

The large value of ξ necessary for maximum noise reduction (8) is ensured by using a coupling mirror having a high transmission T for the signal and idler fields ($T = 6.3\%$, measured cavity finesse of 85 at 1064 nm), whereas the value of L is fixed by the crystal absorption and by the losses at the different interfaces inside the cavity. It is equal to 0.6% (round trip losses), so that ξ reaches a value of 0.91 in this experiment. The mirror transmission for the pump field ($T = 10\%$, measured cavity finesse of 25 at 532 nm) has been chosen to be high enough so that the oscillation threshold I_t (5) is within the reach of the pump laser, and low enough so that, according to the previous discussion, it is always possible to find a suitable cavity length for triply resonant operation without varying another control parameter (see Fig. 8). Let us also mention that, because of the rather large absorption of KTP at 532 nm (more than 4% double pass) a larger cavity finesse would induce spurious heating effects, preventing the OPO from being held triply resonant.

In the experiment, as the cavity is linear, the nonlinear coupling coefficient χ strongly depends on the overlap between the three standing wave patterns inside the crystal [37]. We have therefore used cavity mirrors (from LaserOptiks, Hannover) presenting suitable phaseshifts on reflection to optimize the conversion efficiency and ensure minimum oscillation threshold.

The signal and idler beams are separated by a polarizing beamsplitter, and focussed on InGaAs PIN photodiodes (Epitaxx ETX 300, diameter: 300 μm) tilted by 45% in the polarization plane of the monitored beams in order to reduce the losses by reflection on the photodiode surface. Their quantum efficiency η was measured to be near 0.94 (efficiency at normal incidence: 0.90). All the optical surfaces between the OPO cavity and the detectors are anti-reflection coated. The low frequency part (dc to 30 kHz) of the measured fluctuations is summed (gain balance of the summing electronics better than 1%) and used in the OPO length control. A 180° C power combiner (Minicircuit ZSCJ-2-2) generates the difference between the high frequency part (0.5–20 MHz) of the signal and idler beam fluctuations, suitably preamplified (OEI AH0013 FET preamplifier), which is sent into a spectrum analyser (Tektronix 2753P). The filtering of the low frequency part of the intensity fluctuations has the extra advantage of preventing amplifier saturation resulting from the low frequency excess noise in the observed signals. When the mean intensity measured by each photodiode is 3 mW, the respective amplifier noise, Johnson-noise and shot-noise power contributions scale approximately as 1:2:50, meaning that the electronic noise floor was typically 4 to 12 dB below the signal of interest. Special care was given to the detection balance and linearity, which plays a paramount role in the finally observed quantum noise reduction. The electronic common mode rejection ratio (CMMR) was measured to be −40 dB up to 6 MHz, and −335 dB up to 20 MHz.

The total electrical and optical CMRR (including photodiode imbalance) was measured by modulation of the OPO pump intensity and observation of the resultant modulation peaks in the down-converted beams both individually and by subtraction. It was found to be −35 dB up to 6 MHz

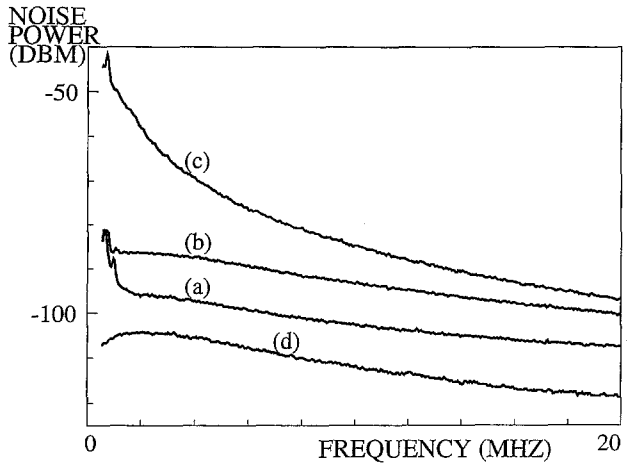

Fig. 9. Recorded noise power spectra (logarithmic scale): (*a*) intensity difference; (*b*) shot noise level; (*c*) single beam intensity; (*d*) electronics noise

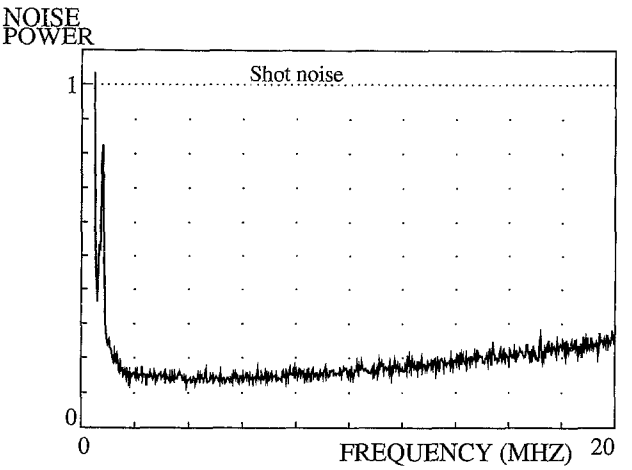

Fig. 10. Normalized intensity difference noise power spectrum computed from curves (*a*), (*b*), (*c*), (*d*) of Fig. 9 (linear scale)

and −30 dB up to 20 MHz. The detection linearity was verified using two methods. The first method was a dc saturation measurement where the twin beam shot-noise power level, measured as described below, was observed to vary linearly with the total intensity incident on the photodiodes. The second was an ac saturation measurement, where one output beam of the OPO was ac modulated, and the resulting modulation peak on the intensity noise power spectrum was observed to vary linearly with the modulation index. Both methods showed excellent linear behaviour for infrared powers up to 4 mW.

Figure 9 shows the various recorded noise power spectra. One observes (curve 9c) a large excess noise on both signal and idler beams (18 dB above shot-noise at 3 MHz), owing to the OPO pumping close to threshold, as expected from theoretical calculations [34, 35]. Even though the intensity noise is expected to be reduced significantly at higher pumping rates, we were confined to work in this conditions to prevent any spurious nonlinearities in the detection of output powers in excess of 3 mW. Curve (9b) gives the standard quantum noise level for intensity difference measurement, which is the shot-noise of a beam having an intensity equal to the sum of the signal and idler mean intensities. As explained in [9], it is obtained by rotating the signal and idler polarizations by 45° C from the polarizer axes using an half-wave plate, thus transforming the polarizing beam-splitter into an ordinary 50% beamsplitter (its shot-noise level has been also checked by looking at the variation of the squeezed noise spectra as a function of variable attenuation inserted in the twin beams [32]). Curve (9a) gives the noise measured in the intensity difference, and curve (9d) the electronic noise floor. Figure 10 displays the intensity difference normalized spectrum, obtained by computing the quantity $[(a)-(d)]/[(b)-(d)]$ from the recorded noise spectra (*a*), (*c*) and (*d*) of Fig. 9, and presented in a linear scale. The noise reduction appears to be significant for frequencies higher than 1 MHz, with a maximum observed noise reduction of $86 \pm 1\%$ (8.5 dB) between 2 and 7 MHz. Quantum noise reduction is expected to occur at frequencies larger than the observed 20 MHz range. Using a Lorentzian fit, following relation (8), we expect a bandwidth at half maximum for squeezing of 45 MHz, which is consistent with the value of the cavity bandwidth. The rise in noise below 1 MHz is due to the residual imbalance in the twin beam intensities which allows the extremely large excess noise of each beam at these frequencies to show up in the difference.

So far the performances of the OPO are not limited by fundamental excess noise sources inherent to the three-wave mixing process in the crystal, but only by the linear losses in the different elements of the OPO. It seems difficult to further increase at the same time the signal-idler mirror transmission T and the pump cavity finesse, because of heating effects due to the pump power build-up in the cavity. A solution that we are presently considering is to further decrease the losses L by reducing the number of intracavity interfaces by using the end faces of the crystal as mirrors. This technique, which would yield very compact and stable sources of non-classical radiation, looks very promising.

If one considers the quantum correlation of the twin beams themselves (thus correcting for the detection process slight inefficiency), one obtains a value of 91% (11 dB) squeezing in the intensity difference. Quantum noise reduction by one order of magnitude in a large frequency range, effective on intense coherent cw light beams, opens the way to ultrasensitive optical measurements, with significant improvements in the signal-to-noise ratios. A first example is given by the generation of single beams with reduced intensity noise, using active control of the intensity of one twin beam from the measurement of the intensity of the other. This method, already demonstrated in [17] with a lower level of twin beam correlation, is closely related to the feedback experiments employing parametric down-conversion [15]. Measurements of very small effects breaking the balance between the intensity of the quantum correlated beams can be performed with a higher sensitivity: linear absorption [22], scattering and polarization rotations [38]. Application to ultrasensitive absorption spectroscopy is, nevertheless, hampered by the difficulty of practically scanning the output frequency of an OPO. This can be solved, for example, by scanning the pump frequency [39]. Another solution is to use Raman processes induced by the signal beam and another laser source, which can be scanned and modulated,

in which one monitors the signal beam absorption in the difference between the transmitted signal intensity and the unaffected idler intensity. A last technique would be to use an OPO which resonates for the pump and idler modes, but not for the signal mode.

4 Discussion

We can now compare the three different generators of twin beams described in Sects. 1, 2 and 3. In the cw regime, the OPO is an intense and narrowband source of non-classical radiation, having both spatial and temporal coherence, analogous in many respects to a laser, whereas parametric fluorescence produces weak, broadband and incoherent non-classical radiation. The high quantum efficiency and low noise photodection systems (even for very weak beams), that have become presently available permit the exploitation of the large measured quantum correlation in both devices. Thus, these two systems are to date the most efficient sources of non-classical radiation, on an equal footing with the current noise suppressed semiconductor lasers [40]. Furthermore, from the experimental point of view they turn out to be rather simple devices: special care must simply be taken to reduce as much as possible all sources of optical losses for the signal and idler beams. The choice between the two systems depend essentially on the specific requirements of the application. For example, when bandwidth considerations prevail and twin photons with extremely short time separation are needed, parametric fluorescence is more advantageous. On the other hand, if the important parameter to optimize is, for example, a signal-to-noise ratio for signals in the MHz range, the parametric oscillator is more convenient. Parametric amplification in the pulsed regime combines many of the features of the two previous systems. It has the advantages of large bandwidth and high intensity, and at the same time it generates output beams with a high degree of spatial and temporal coherence. It is therefore a very promising technique that is likely to provide a versatile source of quantum-correlated light, once the present experimental difficulties are resolved.

Acknowledgements. The results given in this review have been obtained in the framework of the ESPRIT Basic Research Action 3186 NOROS (Quantum Noise Reduction in Optical Systems). Laboratoire de Spectroscopie Hertzienne is laboratoire de l'Ecole Normale Supérieure et de l'Université P.M. Curie, associé au Centre National de la Recherche Scientifique.

References

1. H.J. Kimble, M. Dagenais, L. Mandel: Phys. Rev. Lett. **39**, 691 (1977)
2. R. Short, L. Mandel: Phys. Rev. Lett. **51**, 384 (1983)
3. R.E. Slusher, L.W. Holberg, B. Yurke, J.C. Mertz, J.E. Valley: Phys. Rev. Lett. **55**, 2409 (1985)
4. H.J. Kimble, J.L. Hall, H. Wu: Phys. Rev. Lett. **57**, 2520 (1986)
5. R.E. Slusher, P. Grangier, A. La Porta, B. Yurke, M.J. Potasek: Phys. Rev. Lett. **59**, 2566 (1987)
6. D.C. Burnham, D.L. Weinberg: Phys. Rev. Lett. **25**, 84 (1973)
7. C.K. Hong, L. Mandel: Phys. Rev. Lett. **56**, 58 (1986)
8. J.G. Walker, E. Jakema: Opt. Acta **32**, 1303 (1985)
9. J.G. Rarity, P.R. Tapster, E. Jakeman: Opt. Commun. **62**, 201 (1987)
10. C.K. Hong, S.R. Friberg, L. Mandel: Appl. Opt. **24**, 3877 (1985)
11. S.F. Seward, P.R. Tapster, J.G.Walker, J.G. Rarity: Quantum Opt. **3**, 201 (1991)
12. J.G. Rarity, P.R. Tapster: Phys. Rev. A **45**, 2052 (1992)
13. O. Aytur, P. Kumar: Phys. Rev. Lett. **65**, 1551 (1987)
14. T. Debuisschert, S. Reynaud, A. Heidmann, E. Giacobino, C. Fabre: Quantum Opt. **1**, 3 (1989)
15. P.R. Tapster, J.G. Rarity, J.S. Satchell: Phys. Rev. A **37**, 2963 (1988)
16. A. Heidmann, R.J. Horowicz, S. Reynaud, E. Giacobino, C. Fabre: Phys. Rev. Lett. **59**, 2555 (1987)
17. J. Mertz, A. Heidmann, C. Fabre, E. Giacobino, S. Reynaud: Phys. Rev. Lett. **58**, 2897 (1990)
18. E. Jakeman, J.G. Rarity: Opt. Commun. **56**, 219 (1986)
19. P.R. Tapster, S.F. Seward, J.G. Rarity: Phys. Rev. A **44**, 3266 (1991)
20. M. Xiao, L.A. Wu, H.J. Kimble: Opt. Lett. **13**, 476 (1988)
21. C.D. Nabors, R.M. Shelby: Phys. Rev. A **42**, 556 (1990)
22. I. Abram, R.K. Raj, J.L. Oudar, G. Dolique: Phys. Rev. Lett. **57**, 2516 (1986)
23. P. Kumar, O. Aytur, J. Huang: Phys. Rev. Lett. **64**, 1015 (1990)
24. O. Aytur, P. Kumar: Opt. Lett. **17**, 529 (1992)
25. P.D. Townsend, R. Loudon: Phys. Rev. A **45**, 458 (1992)
26. A. LaPorta, R.E. Slusher: Phys. Rev. A **44**, 2013 (1991)
27. L.A. Lugiato, C. Oldano, C. Fabre, E. Giacobino, R. Horowicz: Nuovo Cimento **10**, 959 (1988)
28. T. Debuisschert: Ph.D. Thesis, Université P.M. Curie, Paris (unpublished 1990)
29. R.C. Eckardt, C.D. Nabors, W.J. Kozlovsky, R.L. Byer: J. Opt. Soc. Am. B **8**, 646 (1991)
30. S. Reynaud: Europhys. Lett. **4**, 427 (1987)
31. C. Fabre, S. Reynaud: Les Houches session 53, ed. by J. Dalibard, J.M. Reynaud (Elsevier 1992)
32. J. Mertz, T. Debuisschert, A. Heidmann, C. Fabre, E. Giacobino: Opt. Lett. **16**, 1234 (1991)
33. C.M. Savage, D.F. Walls: J. Opt. Soc. Am. B **4**, 1514 (1987)
34. G. Björk, Y. Yamamoto: Phys. Rev. A **37**, 125 (1988)
35. C. Fabre, E. Giacobino, A, Heidmann, S. Reynaud: J. Phys. (Paris) **50**, 1209 (1989)
36. C. Fabre, E. Giacobino, A. Heidmann, L. Lugiato, S. Reynaud, M. Vadacchino, Wang Kaige: J. Opt. Soc. Am. B **7**, 2132 (1990)
37. H.J. Kimble, J.L. Hall: *Quantum Optics IV*, ed. by G. Harvey, D. Walls Springer Proc. Phys., Vol. **12** (Springer, Berlin, Heidelberg 1986)
38. J. Snyder, E. Giacobino, C. Fabre, A. Heidmann, M. Ducloy: J. Opt. Soc. Am. B **7**, 2132 (1990)
39. E.S. Polzik, J. Carri, H.J. Kimble: In OSA Annual Meeting Technical Digest, Vol. 17 (Optical Society of America, Washington, DC 1991) p. 29
40. W.H. Richardson, S. Machida, Y. Yamamoto: Phys. Rev. Lett. **66**, 2867 (1991)